Pathological and Physiological High-Frequency Oscillations on Whole-Brain Noninvasive Recordings: Comparing Healthy Children and Patients with Epilepsy

Lorenzo Fabbri[1,2], Cecilia Liberati[3], Shannon Conrad[1], Deniz Aygun[3], Steven Stufflebeam[4], Phillip L Pearl[3], M. Scott Perry[1], EleonoraTamilia[5], Christos Papadelis[1,2,6]

1. Jane and John Justin Institute for Mind Health Neurosciences Center, Cook Children's Health Care System, Fort Worth, TX, USA. 2. Department of Bioengineering, University of Texas at Arlington, Arlington, TX, USA. 3. Division of Epilepsy and Clinical Neurophysiology, Department of Neurology, Boston Children's Hospital, Harvard Medical School, Boston, MA, USA. 4. Athinoula A. Martinos Center for Biomedical Imaging, Massachusetts General Hospital & Harvard Medical School, Charlestown, MA, USA. 5. Division of Newborn Medicine, Department of Medicine, Boston Children's Hospital, Harvard Medical School, Boston, MA, USA. 6. School of Medicine, Texas Christian University, Forth Worth, TX, USA.

Background & Rationale

- For children with **drug-resistant epilepsy (DRE)**, surgery is the best available treatment to achieve seizure freedom. The success of epilepsy surgery depends on the precise delineation of the **epileptogenic zone (EZ)**, the brain area that is indispensable for the generation of seizures.
- **High-Frequency Oscillations (HFO)** are among the most promising interictal biomarkers of epileptogenicity in **DRE**, yet their clinical value is still debated due to the presence of **physiological HFOs (*physHFOs*)** in healthy brain regions.
- Previous studies have used **intracranial EEG (iEEG)** data to separate physHFOs from **pathological HFOs (*pathHFOs*)** but suffered from the inability to obtain full head coverage and to record data from **typically developing (TD)** controls.
- Here, we **aim** to use full-head noninvasive methods to: **(a)** generate the first cortical map of physHFOs in the normal human brain; **(b)** identify differences between the HFOs generated by the healthy and the epileptic brain; and **(c)** developing an automated classifier of ***physHFOs***.

Methods

- **Patients:** 26 DRE (age: 13.6 ± 3.0 years; 12 males) and 21 TD (age: 11.5 ± 3.6 years; 9 males) patients.
- **Recordings:** We analyzed simultaneous magnetoencephalography (MEG; 306 sensors) and high-density EEG (HD-EEG; 256 channels) sampled at ≥ 1000 Hz.
- **HFOs:** We detected HFOs (ripples: 80-160 Hz) on MEG and HD-EEG separately using an automated detection algorithm followed by visual review and localized their cortical sources using electric and magnetic source imaging **(Fig 1A).** For each HFO, we extracted a set of temporal, spatial, morphological, and spectral features **(Fig 1B)**, and compared between **TD and DRE** groups (Wilcoxon rank-sum test).
- **Classifier:** The extracted features were used to train and test (10-fold cross-validation) a **k-nearest-neighbor (kNN)** classifier for discriminating ***physHFOs*** and ***pathHFOs***.
- For all statistical tests, we considered significance at the level of p<0.05.

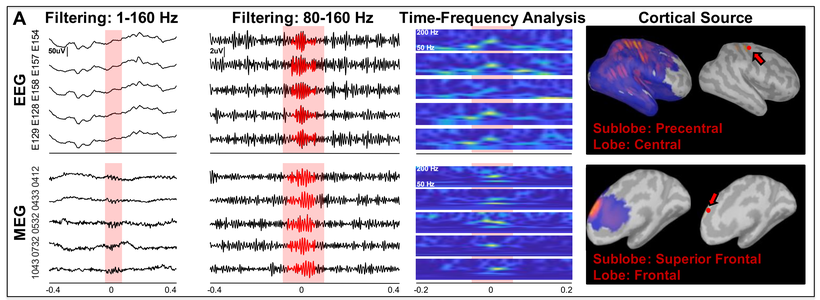

B Feature	Definition
Peak Frequency	Average of the peak frequency across the involved channels (channels where the HFO is detected)
Frequency Variability	Coefficient of Variation (COV) of the peak frequency across the involved channels
Power Ratio	Ratio between power of the HFO and the surrounding background (average across involved channels)
Duration	Interval between the HFO onset and offset
Duration Variability	Coefficient of Variation (COV) of the duration of HFOs across all the involved channels
Propagation Latency	Average latency between consecutive HFOs across the involved channels
Amplitude	Maximum of the envelope amplitude during the HFO (average across the involved channels)
Amplitude Variability	COV of the maximum envelope amplitude during the HFO (across the involved channels)
Channel extent	Number of channels involved in the HFO event
Source extent	Number of active cortical vertices during the HFO (based on source imaging)

Figure 1. (A) Physiological HFO in EEG (top) and MEG (bottom). Each scenario shows: **(i)** signals filtered between 1 and 160 Hz for artifacts visualization; **(ii)** signals filtered between 80 and 160 Hz on an expanded timescale (ripple time windows in red); **(iii)** time-frequency analysis (TFA) showing the ripple "island", and **(iv)** source localization on the subject's 3D cortical surface of each ripple with highlighted maximum (red). **(B)** Comprehensive list of features. Spectral (green), Temporal (blue), Morphological (yellow), and Spatial (red).

Results

- We found more HFOs on HD-EEG than MEG in both the TD (235 vs. 74 HFOs; 76% vs. 24%) and DRE group (378 vs. 223 HFOs; 63% vs. 37%).
- For HD-EEG, HFOs in the TD group had a shorter and less variable duration than the DRE group (**Fig 2A-B**, p<0.001), more variable frequency (**Fig 2C**, p<0.001), greater propagation latency (**Fig 2D**, p<0.001), and lower amplitude (**Fig 2E**, p<0.001).
- For MEG, HFOs in the TD group had a shorter and less variable duration than the DRE group (**Fig 2A-B**, p<0.01), more variable frequency (**Fig 2C**, p<0.05), lower propagation latency (**Fig 2D**, p<0.01), and higher amplitude (**Fig 2E**, p<0.001).
- For both the TD and DRE groups, MEG HFOs had a higher frequency than HD-EEG HFOs (**Fig 2F**, p<0.001) while HD-EEG HFOs had a larger spatial extent at the sensor level than MEG HFOs (**Fig 2G**, p<0.001). For the DRE group, MEG HFOs had a weaker power content than HD-EEG HFOs (**Fig 2H**, p<0.05), while the opposite was true for the TD group (**Fig 2H**, p<0.01).
- We generated 3D maps of physHFOs in the normal pediatric cortex demonstrating high rates in the somatosensory area for both HD-EEG and MEG (**Fig 3A**).
- Our kNN classifier showed a 74% and 78% accuracy in discriminating the EEG/MEG-HFOs from the TD and DRE group (**Fig 3B**; p<0.001) and correctly classified 82% of the pathHFOs for both EEG and MEG.

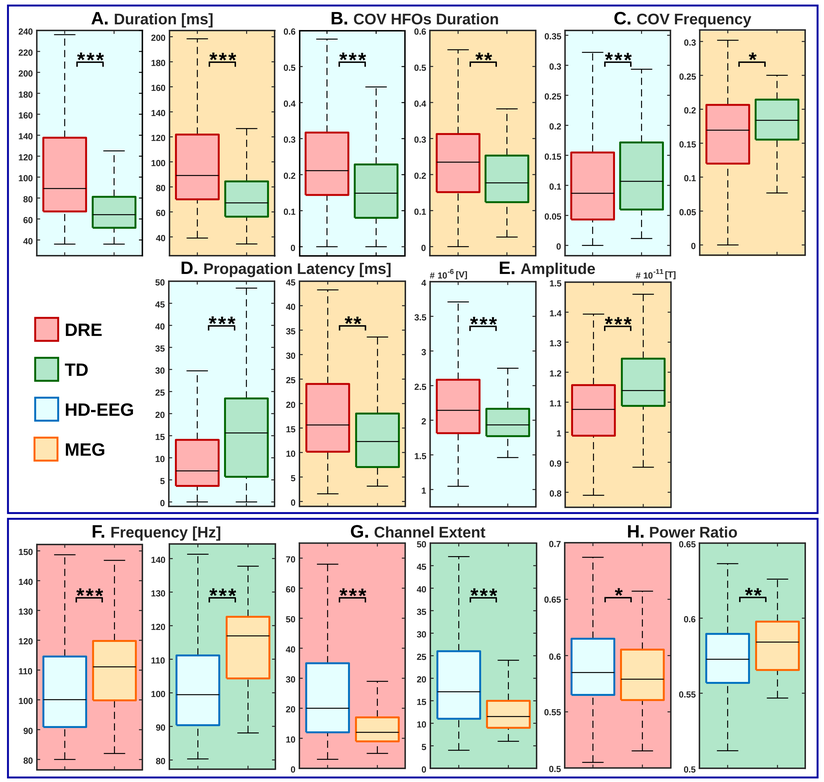

Figure 2. HFOs features on HD-EEG and MEG: boxplots of the comparison between TD (green) and DRE (red) groups (top). Boxplots of the comparison between HD-EEG (blue) and MEG (orange) groups (bottom) (* p value ≤ 0.05; ** ≤ 0.01; *** ≤ 0.001).

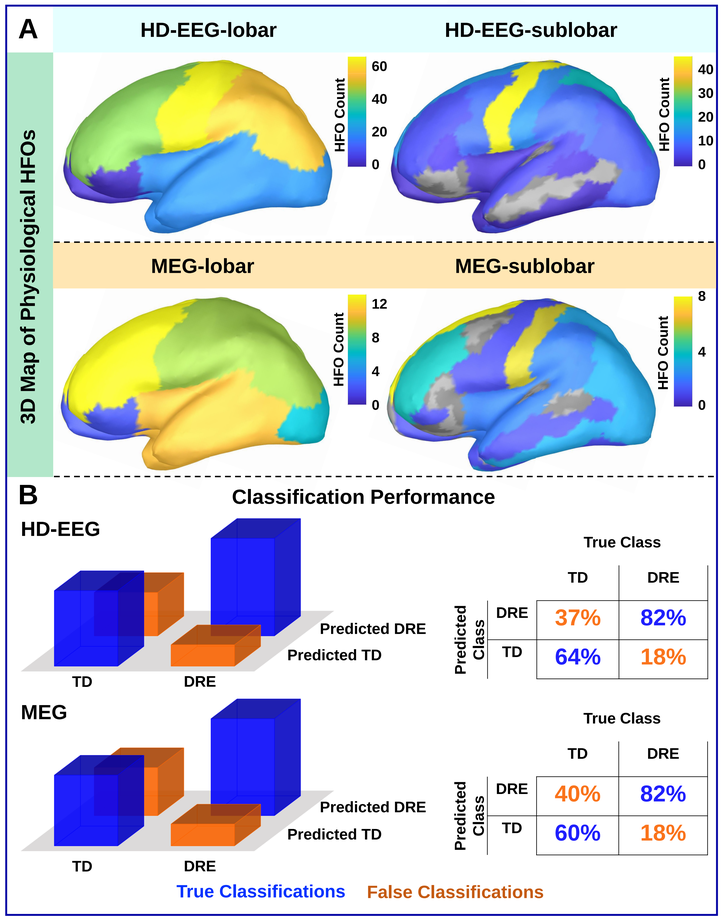

Figure 3. (A) Anatomical Distribution of Physiological HD-EEG and MEG HFOs on the inflated cortex. HFOs were assigned to a lobar and sublobar region based on the Desikan-Killiany atlas (34 sublobes) and counted across the whole cohort (subjects for EEG and for MEG). **(B) Performance of the kNN classifier**

Conclusions

We exhibit here the **first 3D cortical map of physHFOs in the normal pediatric brain estimated using HD-EEG and MEG** and presented a comprehensive set of features that can distinguish HFOs generated by healthy and epileptic brain with a 74% and 78% accuracy on HD-EEG and MEG respectively.

Funding

National Institute of Neurological Disorders & Stroke (RO1NS104116-01A1, PI: C. Papadelis; and R21NS101373-01A1, PIs: C. Papadelis and S. Stufflebeam).